

pubs.acs.org/JPCB Article

Cyclopropane as an Unsaturation "Effect Isostere": Lowering the Melting Points in Lipid-like Ionic Liquids

Richard A. O'Brien,* Patrick C. Hillesheim, Mohammad Soltani, Kelly J. Badilla-Nunez, Ben Siu, Muhammadiqboli Musozoda, Kevin N. West, James H. Davis, Jr.,* and Arsalan Mirjafari*



Cite This: J. Phys. Chem. B 2023, 127, 1429-1442



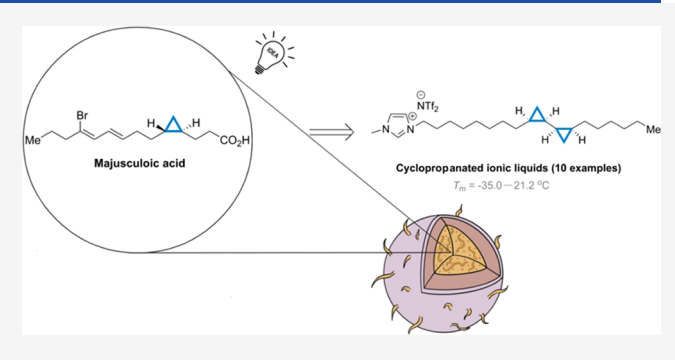
ACCESS I

III Metrics & More

Article Recommendations

Supporting Information

ABSTRACT: The replacement of unsaturation with a cyclopropane motif as a (bio)isostere is a widespread strategy in bacteria to tune the fluidity of lipid bilayers and protect membranes when exposed to adverse environmental conditions, e.g., high temperature, low pH, etc. Inspired by this phenomenon, we herein address the relative effect of the cyclopropanation, both cis and trans configurations, on melting points, packing efficiency, and order of a series of lipid-like ionic liquids via a combination of thermophysical analysis, X-ray crystallography, and computational modeling. The data indicate there is considerable structural latitude possible when designing highly lipophilic ionic liquids that exhibit low melting points. While cyclopropanation of the lipid-like ionic liquids



provides more resistance to aerobic degradation than their olefin analogs, the impact on the melting point decrease is not as pronounced. Our results demonstrate that incorporating one or more cyclopropyl moieties in long aliphatic chains of imidazoliumbased ionic liquids is highly effective in lowering the melting points of such materials relative to their counterparts bearing linear, saturated, or thioether side chains. It is shown that the cyclopropane moiety effectively disrupts packing, favoring formation of gauche conformer in the side chains, resulting in enhancement of fluidity. This was irrespective of the configuration of the methylene bridge, although marked differences in the effect of cis- and trans-monocyclopropanated ILs on the melting points were observed.

INTRODUCTION

For 20-odd years, ionic liquids (ILs) have been subjects of intense scrutiny by a broad spectrum of academic and industrial chemists alike, and large-scale, industrial utilization of them have been recently established. 2,3 Two decades after the initial report of air-and water-stable imidazolium-based ILs, we are now in the midst of a new wave wherein novel ILs are constantly being developed and rapidly adopted across scientific disciplines. Concomitantly, the physical properties of ILs have been of particular interest, particularly concerning their melting points and miscibility (or lack thereof) with various molecular solvents.⁵ Imidazolium-based ILs are central in generating publications containing our knowledge about these materials. $^{6-12}$ The melting point $(T_{\rm m})$ values of salts of the former cation class have been systematically studied as a function of several variables, although the chief foci of such studies have been concerned with (i) the associated anion of the salt and (ii) with the precise nature of the N'-bonded organic appendages of the cation.¹³

The nature of the side chains tethered to cations of imidazolium salts profoundly influences their fluidity/liquefaction behaviors. Several of the earliest-and still most valuable-studies on the liquefaction of ILs established that increasing the length of one of the alkyl groups results in the

lowering of $T_{\rm m}$ values. ^{14–17} This trend holds true when moving from C1 to about C5, at which there is a leveling-off until a chain length of ca. C₇ is reached. At this point, there is a sharp uptick in melting points that quickly grows to exceed ambient temperature (Figure 1). Due to the decades of work to generate this figure and data, several critical structural design principles of ILs have emerged, highlighting the importance of symmetry, steric, and conformational flexibility of the alkyl chains. 18 Consequently, it seemed unlikely that it would be possible to prepare ILs with ever-increasing lipophilic character, eventually making their melting points too high to be used in some of the envisioned applications. 19-21

However, as a group with a longstanding interest in rationally designing and preparing ILs to have new functions (molecular behavior), we saw this dilemma as posing an interesting challenge. Taking our cue from nature's approach, we introduced the concept of lipid-like (or lipidic) ILs 12 years

Received: November 8, 2022 Revised: January 11, 2023 Published: February 6, 2023





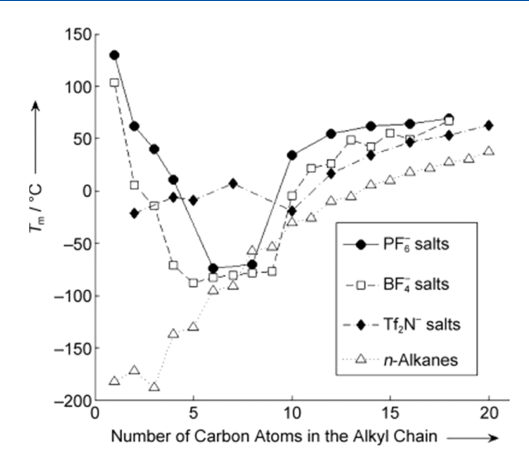


Figure 1. Effect of alkyl-chain length on $T_{\rm m}$ in 1-alkyl-3-methylimidazolium salts and the corresponding n-alkanes. Reproduced from ref 6 with permission from Jon Wiley and Sons.

ago by focusing on its raison d'être: the creation of ILs that are highly lipophilic, low-melting, and potentially bio-innocuous. Lipid-like ILs are a multifarious class of bioinspired materials that include saturated, unsaturated, linear, branched, or functionalized (e.g., ether, thioether) lipidic side chains while retaining melting points that are below room temperature.² Our first efforts in this direction were successful and resulted in (among other things) the synthesis of ene-bearing imidazolium-type lipid-like ILs.6 Initially, we set out to establish that by way of incorporating unsaturation (particularly cis) in the long imidazolium ion side chains, we could create salts of that cation type with a high degree of lipophilic structural character that nevertheless manifested low $T_{\rm m}$. The inspiration for this strategy was a biological phenomenon known as homeoviscous adaptation (HVA),²³ in which the composition of cell membrane lipid bilayer of certain organisms varies on a seasonal basis to ensure optimal fluidity. The proper function of the lipid bilayer is closely tied to its fluidity, which is often quantified by reference to $T_{\rm m}$ —i.e., increased fluidity = lower $T_{\rm m}$. Consider that phospholipids with unsaturated side chains (i.e., from oleic acid, linoleic acid, etc.) have much lower $T_{\rm m}$ values than counterparts with saturated (i.e., stearic acid) side chains. The concept of lipid-like ILs worked quite well, and imidazolium-type ILs had $T_{\rm m}$ values as low as $-46.8~^{\circ}{\rm C}$ while featuring 18-carbon alkyl side (Figure 2). We continued to build on those preliminary results, and we exploited the same strategy but applied it to ILs with ammonium²⁴ and methimazolium¹¹ cation headgroups, which were likewise successful.

While the former efforts were in progress, an unanticipated consequence of the side-chain unsaturation was gradually making itself apparent—the oxidative cleavage (albeit very slowly) of the side chain when the IL was stored and handled under air in lieu of an inert atmosphere. In retrospect, the behavior should have been expected; naturally occurring unsaturated fats eventually become rancid for the same reason. Moreover, while we established that (taking a cue from the food industry) this side-chain cleavage in the ILs could be prevented by the addition of small amounts of the antioxidant butylated hydroxytoluene (BHT) to them, we nevertheless set out to identify other side-chain modifications that might similarly "kink" the lipidic tails (viz., local cis geometry being responsible for the $T_{\rm m}$ depression effect), but without coincident air sensitivity. Although side-chain oxidative

Figure 2. Influence of a "kink" in the side chain of a C18-based saturated (strearyl) and unsaturated (linoleyl) ILs.⁶

cleavage may be advantageous from a biodegradability perspective, it might complicate their use in specific practical applications. As such, we sought to identify a scission-resistant "effect isostere" that would alter the fluidity of lipidic materials in a similar manner to olefins while retaining their lipophilicity.

Subsequently, two alternative $T_{\rm m}$ depression approaches were found to be highly useful: One of these was the replacement of the double bonds by midchain thioether groups, and we have published several papers detailing various aspects of the chemistry of those ILs. 10,25 Still, thioethers are susceptible to slow oxidation to sulfoxides, although this process does not lead to molecular cleavage. The second approach involved replacing the double bond with a cisoid cyclopropyl moiety, a strategy used by numerous organisms that utilize cyclopropanated lipids to depress $T_{\rm m}$ and modulate cell membrane fluidity (Figure 3). It is commonly accepted that the presence of cyclopropane fatty acids enhances the chemical and physical stability of membranes against undesired compounds, e.g., superoxide, singlet oxygen, ozonolysis, and oxidative stress.²⁶ However, we terminated our proof-ofconcept study after preparing and studying two compounds (C16 based),9 since we discovered that synthesizing monocyclopropanated ILs was considerably more complex than the thioether-containing materials. Nevertheless, the monocyclopropanated IL did prove to have a melting point lower than that of the corresponding linear, saturated-sidechain IL; that is, the concept of $T_{\rm m}$ depression via side-chain cyclopropanation was (at least for the one example) validated.

While the cyclopropane is a highly strained entity, the angle strain of the three-membered ring renders this group an appealing structural unit for many natural fatty acids and natural products²⁷ as well as for the production of energy-dense fuels for high energy-demanding applications such as aviation and rocketry (Figure 3).²⁸ To understand a cyclopropane ring's effect on lipid bilayer fluidity, Poger and Mark examined lipid packing, chain order, and conformational preference of the cyclopropanated lipid bilayers via MD simulations.²⁹ They found that cyclopropane fatty acids enhance the fluidity of lipid bilayers via altering lipid packing and favor the formation of *gauche* defects in the chains while increasing the degree of order along the chains, preventing the rotation of the bonds surrounding the cyclopropane motif.

Anderson and co-workers recently described the use of lipidlike ILs provided by our group as stationary phases in the GC

Cardiolipins with cyclopropanate fatty acids

Figure 3. Examples of naturally occurring and useful compounds containing cyclopropane fatty acid motifs. Syntin is a synthetic fuel, which was used as a rocket fuel for the Soyuz and Proton. ²⁸ N.B.: no absolute configuration of cyclopropane moieties implied for Jawsamycin, U-106305, and cardiolipins derivative for the sake of clarity.

analysis of kerosene.³⁰ The results of that study were encouraging insofar as separating nonpolar components at high operating temperatures is concerned. Among the specific ILs evaluated in their work was the monocyclopropanated IL we had described earlier.⁹ Significantly, it not only proved to be a useful stationary phase for the separation but was also found to be the most thermally stable of the lipid-like ILs evaluated in that role. Encouraged by these results, we reconsidered our earlier abandonment of further cyclopropanated IL development and prepared a series of 10 mono- and polycyclopropanated ILs (2-CP, 4-CP-10-CP, 12-CP, 13-CP), in a six-step process from high-purity fatty acids for the evaluation of their thermophysical properties (Figure 4). We hypothesize that cyclopropane fatty acids can serve as adaptable and practical "tutors" of lipid-like IL design, offering

valuable insights on structural components consistent with simultaneous low-temperature fluidity and high lipophilicity. Notably, to achieve the highest fluidity possible, we strategically placed cyclopropane rings in the nature-selected C9—C10 or C11—C12 symmetry-breaking positions of several ILs, e.g., 5-CP, 6-CP, or 9-CP (Figure 4).

For the sake of clarity in discussing the properties of the new ILs, and to facilitate their comparison to their molecular analogs, the following convention is used in distinguishing between them: the compound number, as noted in Tables 1–3, defines the base alkane or alkene chain along with the unsaturation pattern. The suffix following the number describes whether the compound is a saturated/unsaturated IL (-AL), a cyclopropanated IL (-CP), a molecular fatty acid (-FA), or a molecular methyl ester of the fatty acid (-ME). For

$$\begin{array}{c} \text{Me} \\ \text{Me} \\$$

Figure 4. Top: Synthetic pathway of monocyclopropanated IL 5-CP as a representative method for the synthesis of cyclopropanated IL analogs. The olefin cyclopropanation occurred through the Simmons–Smith reaction. Bottom: Structures of synthesized cyclopropanated ILs (CPs). The counteranion is NTf_2^- that was omitted for clarity.

example, 7-CP represents an 1-alkyl-3-methylimidazolium bistriflimide salt where the side chain has base structure 7 (a C18 chain with a *trans* double bond at the 9–10 position, which has been cyclopropanated) while **5-ME** would represent the methyl ester of a C18 fatty acid with a *cis* double bond in the 9-10 position.

■ RESULTS AND DISCUSSION

The new ILs were evaluated by differential scanning calorimetry (DSC), and the resulting melting points, enthalpies, and entropies of fusion are listed in Tables 1 and 2; uncertainties are calculated as the standard deviation of the mean. To understand the effect of cyclopropanation on the melting points of these compounds, the $T_{\rm m}$ values of the parent

series of saturated/unsaturated of ILs (-AL), their cyclopropanated counterparts (-CP) (Figure 4), the analogous saturated/unsaturated fatty acid (-FA), and the methyl ester of the fatty acid (-ME) are shown in Table 1. Two trends emerge from this analysis:

The first trend is that the melting points of the ILs increase upon conversion from the unsaturated species to the cyclopropanated species, proportional to the degree of cyclopropanation. As demonstrated in Table 1, the cyclopropane-induced "kink" in the aliphatic side chain plays a crucial role in drastically lowering the chain order and packing efficiency and the subsequent $T_{\rm m}$ values of the ILs. The average $T_{\rm m}$ increase for species converted from a single cis unsaturation to a single cis cyclopropanation is 8.0 °C, for conversion for

Table 1. T_m Values for Saturated, ene-Bearing, Cyclopropanated ILs Along with Their Fatty Acid and Methyl Ester Analogs

| | | T_{m} (°C) | | | |
|----------------|----------------------|-----------------------|-----------------------|------------------|--------------------|
| base structure | appendage type | alkyl/alkenyl (-AL) | cyclopropanated (-CP) | fatty acid (-FA) | methyl ester (-ME) |
| 1 | C16:0 | 46.9 | | 63.5 | 33.5 |
| 2 | C16:1, cis 9 | -22.0 | -35.0 | 0.5 | -33.9 |
| 3 | C18:0 | 53.5 | | 69.6 | 38.9 |
| 4 | C18:1, cis 6 | -2.2 | -1.5 | 29.8 | |
| 5 | C18:1, cis 9 | -20.9 | -8.6 | 16.2 | -19.6 |
| 6 | C18:1, cis 11 | -9.8 | 8.3 | 12.0 | -24.3 |
| 7 | C18:1, trans 9 | 16.0 | 21.2 | 43.7 | 10.3 |
| 8 | C18:2, cis 9, 12 | -46.8 | -27.7 | -6.5 | -35.0 |
| 9 | C18:2, cis 9, 11 | -48.6 | -25.5 | 22.0 | |
| 10 | C18:3, cis 9, 12, 15 | -80.0 | -27.8 | -11.0 | |
| 11 | C20:0 | 62.5 | | 75.5 | 54.0 |
| 12 | C20:1, cis 11 | 4.2 | 7.7 | 23.5 | -34.0 |
| 13 | C20:2, cis 11, 14 | -38.9 | $-7.5 (T_{\rm g})$ | | |

Table 2. Comparison of Melting Points, Enthalpy, and Entropy of Fusion Values

| compound | $T_{\rm m}$ (°C) | $\Delta H (kJ/g)$ | $\Delta S_{\text{fus}} (J/g \text{ K})$ |
|----------|------------------|-------------------|---|
| 2-CP | -35.0 ± 0.3 | 20.1 ± 0.8 | 84 ± 4 |
| 2-ME-CP | -36.7 ± 0.2 | 47.2 ± 0.62 | 200 ± 4 |
| 4-CP | -1.5 ± 0.2 | 37.8 ± 1.5 | 139 ± 28 |
| 5-CP | -57.21 | 2.133 | 10 |
| 6-CP | 8.3 ± 0.2 | 58.6 ± 1.5 | 208 ± 10 |
| 8-CP | -27.8 | | |
| 9-AL | -48.64 | 1.74 | 8 |
| 9-CP | -25.5 ± 0.5 | 0.68 ± 0.04 | 2.7 ± 0.2 |
| 10-CP | -27.8 ± 0.1 | 0.61 ± 0.03 | 2.48 ± 0.12 |
| 12-CP | 7.7 ± 0.4 | 55.5 ± 3.4 | 198 ± 23 |
| 13-AL | -38.87 | 1.359 | 6 |
| 13-CP | -7.5 ± 0.6 | 0.71 ± 0.11 | 2.7 ± 0.6 |
| | | | |

doubly unsaturated species to double cyclopropanated species is \sim 25 °C, and the increase for the tri-unsaturated species is 52 °C. This is consistent with the idea that cyclopropanation decreases the degrees of freedom of the chain, limiting mobility in the liquid phase and decreasing the entropy of the liquid, which in turn decreases the enthalpy of fusion and increases the $T_{\rm m}$. Similar effect is observed for the gel-to-liquidcrystalline phase transition cyclopropane fatty acids.³¹ When both fatty acids in a phospholipid bilayer are identical, cyclopropanated, or unsaturated, the phase transition takes place at a higher temperature for cyclopropane-containing bilayers, indicating that they have a lower degree of fluidity. In contrast, the cyclopropanated moiety still frustrates packing in the solid phase, resulting in melting points for the cyclopropanated species which, though higher than their more thermally and oxidatively labile unsaturated analogs, are markedly lower than their saturated counterparts. The same trend can be observed for cyclopropane fatty acids, which are more ordered relative to their analogous unsaturated chains (Table 1). Thus, cyclopropanation of unsaturated lipid-like ILs plainly provides a means to replace the less stable alkene modules while still maintaining relatively low melting points. Even so, there is an outlier from the foregoing trend (2-CP), which has a melting point 13 °C lower than its unsaturated counterpart. We postulate that this deviation is likely a result of the shorter chain in 2 (C16 vs C18 or C20), which results in the cyclopropyl motif being closer to the end of the chain. This would then further frustrate packing in the solid phase and lead

to fewer dispersion force interactions due to the shorter chain length. Like fatty acids, the stereochemistry of the cyclopropane ring has a determining impact on the degree of fluidity of the ILs (Table 1). That is, *cis*-cyclopropanated ILs (5-CP) tend to be less ordered than its *trans* 7-CP isomer with $\Delta T_{\rm m}$ of 29.8 °C.

The second trend can be seen by examining the enthalpies of fusion (ΔS_{fus}) shown in Table 2. We note that the measured ΔS_{fus} of compounds 8-CP, 9-CP, 10-CP, and 13-CP, all of which are polycyclopropanated species, are much lower than values common for similar species or ordered solids in general. Such values would indicate the possibility of a glass transition (second-order phase transition); however, the shape of the DSC curves of these species is more similar to those observed for a first-order phase transition. To account for this behavior, we posit that due to frustrated packing in the solid phase, only a portion of the sample is able to attain its lowest-energyordered structure, with the bulk of the sample adopting a disordered glassy structure. This, then, results in a sharp endothermic signal from only a small portion of the sample. To test this hypothesis, we measured the ΔS_{fus} of a sample of 10-CP after cooling from a liquid with both high and low cooling rates (20 and 1 °C/min) to potentially induce different levels of crystallinity based on the thermal history of the sample. In doing so, the enthalpies of fusion (ΔH_{fus}) differed by ~7%, which is ca. two times higher than the standard uncertainty for experiments where the thermal history of the samples was the same (Table 2). Although further study of this behavior is necessary, this further indicates the presence of significant packing frustration resulting from the inclusion of cyclopropane moieties in these species.

With the new data from this work, we sought to compare the effect of saturated, unsaturated, cyclopropanated, and thioether moieties embedded within the long aliphatic chains of the imidazolium-based ILs as shown in Table 3. We have spent the past decade studying the effect of structural modifications in the aliphatic chain framework upon the $T_{\rm m}$ of IL materials. Together, the findings provide useful insights on characteristics and correlations that are consistent with obtaining low $T_{\rm m}$ values in salts with lipid-like cation appendages — features that are not apparent from our earlier studies. For our comparison, we look at the C_{18} -based ILs with structural differences in the C9–C10 position of the aliphatic chain as depicted in Figure 5. Indeed, compared to the relevant saturated IL standards 1, 3, or 11, cyclopropanation and unsaturation bring about a radical

Table 3. Comparison of $T_{\rm m}$ Values for C16, C18, and C20-Based ILs with Functionalization at Various Locations Within the Aliphatic Chain

| base structure | chain length | functional group | $T_{\rm m}$ (°C) |
|----------------|--------------|-----------------------------|-------------------|
| 1-AL | C16:0 | | 46.9 ⁶ |
| 2-AL | C16:1 | olefin, cis 9-10 | -22.0^{6} |
| 2-CP | C16 | cyclopropyl, cis 9-10 | -35.0 |
| | C16 | thioether, 9[S] | -2.8^{25} |
| 3-AL | C18:0 | | 53.5^{6} |
| 4-AL | C18:1 | olefin, cis 6-7 | -2.2^{6} |
| 4-CP | C18 | cyclopropyl, cis 6-7 | -1.5 |
| | C18 | thioether, 6[S] | -11.3^{25} |
| | C18 | thioether, 6[S], 7-Me | -27.7^{10} |
| 5-AL | C18:1 | olefin, cis 9-10 | -20.9^{6} |
| 7-AL | C18:1 | olefin, trans 9-10 | 16.0^{6} |
| 5-CP | C18 | cyclopropyl, cis 9-10 | -8.6^{9} |
| 7-CP | C18 | C18 cyclopropyl, trans 9-10 | |
| | C18 | thioether, 9[S] | 24.5^{25} |
| | C18 | thioether 9[S], 10-Me | 1.9^{10} |
| 6-AL | C18 | olefin, cis 11-12 | -9.8^{6} |
| 6-CP | C18 | cyclopropyl, cis 11-12 | 8.3 |
| | C18 | thioether, 11[S] | 27.0^{25} |
| 11-AL | C20:0 | | 62.5^{6} |
| 12-AL | C20:1 | olefin, cis 11-12 | 4.26 |
| 12-CP | C20 | cyclopropyl, cis 11-12 | 7.7 |
| | C20 | thioether, 11[S] | 22.5^{25} |

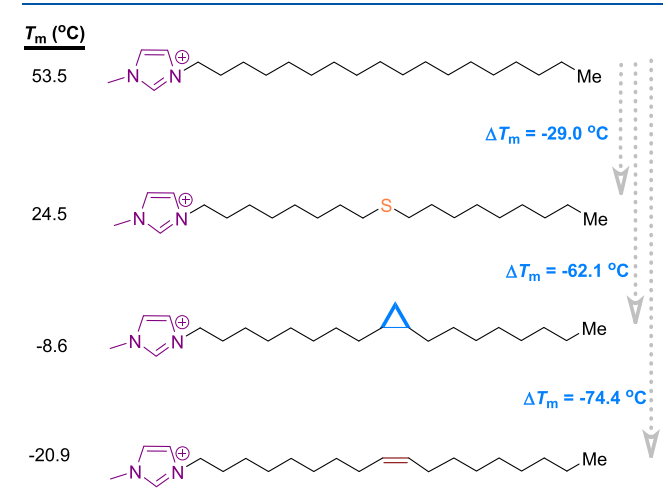


Figure 5. $\Delta T_{\rm m}$ relationships among three generations of lipid-like ILs. The NTf₂⁻ anion was omitted for clarity.

 $T_{\rm m}$ decrease on a same-chain-length basis. This effect closely resembles that observed for the analogous C₁₈ fatty acids and their corresponding methyl esters. The saturated IL (2-AL) yielded a $T_{\rm m}$ value of 53.5 °C while the unsaturated ILs gave $T_{\rm m}$ values of -20.9 °C (cis, 5-AL) and 16.0 °C (trans, 7-AL), which provided $\Delta T_{\rm m}$ of 74.4 and 37.5 °C, respectively. Furthermore, the cis and trans stereoisomers (5-AL and 7-AL) provide additional insight into the effect of the "kink" for the starting oleyl methyl ester 5-ME ($T_{\rm m}$ = -19.6 °C) and the cyclopropanated methyl ester 5-ME whereas the trans stereoisomer 7-ME induces only a mild "kink" into the chain $(T_{\rm m} = 10.3 \, ^{\circ}\text{C})$, which mimics the side chain structure of the stearyl methyl ester 3-ME. Notably, the $T_{\rm m}$ gap for the unsaturated/cyclopropanated pairs 4-AL/4-CP, 5-AL/4-CP, and 7-AL/4-CP are modest (i.e., $\Delta T_{\rm m}$ values are 0.7, 12.3, and 5.2 °C, respectively), indicating that the addition of a single methylene bridge had the same effect on packing, irrespective of its configuration. As expected, comparison of the IL with the saturated alkyl chain (3-AL) to its cyclopropanated analog (5-CP) yields a $\Delta T_{\rm m}$ of 62.1 °C, which illustrates the effect of the cyclopropyl moiety on the packing efficiency and chain order. Marked differences in the effect of cis- and trans-monocyclopropanated ILs were also observed (vide supra). In line with our previous observations, the parent fatty acids have consistently higher $T_{\rm m}$ than their analogous cyclopropanated ILs, mostly due to the presence of the bulky asymmetrical imidazolium headgroup, which prohibits the ILs from interacting as closely together as the parent fatty acids.

Moreover, incorporation of a thioether linkage into the C18 chain strategically at the 9 position (9[S]) via the thiol—ene click reaction 32 yielded a $T_{\rm m}$ = 24.5 °C, with a structure similar to the *trans* cyclopropanated IL 7-CP ($T_{\rm m}$ = 21.2 °C). Our results indicate that cyclopropanated ILs are in general less ordered than the analogous thioether-functionalized ILs (Table 3). Branching at the 10 position on the previously mentioned 9[S] IL lowers the $T_{\rm m}$ to 1.9 °C. It is apparent that introducing branching into a somewhat linear structure of the thioether linkage provides an intermediate $T_{\rm m}$ depression, somewhere between the oleyl-based IL 5-AL and the cyclopropanated trans IL 7-CP.

Seeking greater insights into structure–fluidity correlation, we concluded that X-ray studies of a representative cyclopropanated IL might provide deeper insight into the nature of the structure and the influence upon the packing, conformational preference, and chain order. However, despite considerable effort, we were unable to isolate a cyclopropanated IL in single-crystalline form. Consequently, we made a cyclopropanated salt with progressively shorter-chained analog (C6), paired with Ph_4B^- anion, that was suitably single crystalline at room temperature for analysis. The salt, 14-CP, was then studied by X-ray diffraction (Figure 6). The kinking

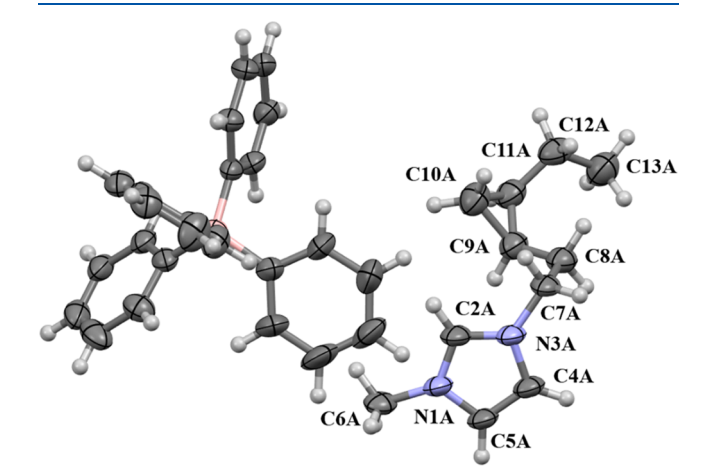


Figure 6. Asymmetric unit of compound **14-CP** shown with 50% probability ellipsoids. Labeling shown for clarity. Only the major portion of the disorder (A) is shown. Carbon = gray; nitrogen = blue; boron = pink; hydrogen = white.

induced by the cyclopropane is clear, and the overall irregular side-chain orientations in this cation are likely representative of their longer-chain counterparts. As can be seen in Figure 7, the *cis* cyclopropyl moiety forces a bend within the alkyl chain and disrupts the long-range packing within the crystalline state. Further, on examining the X-ray structure, it is visually

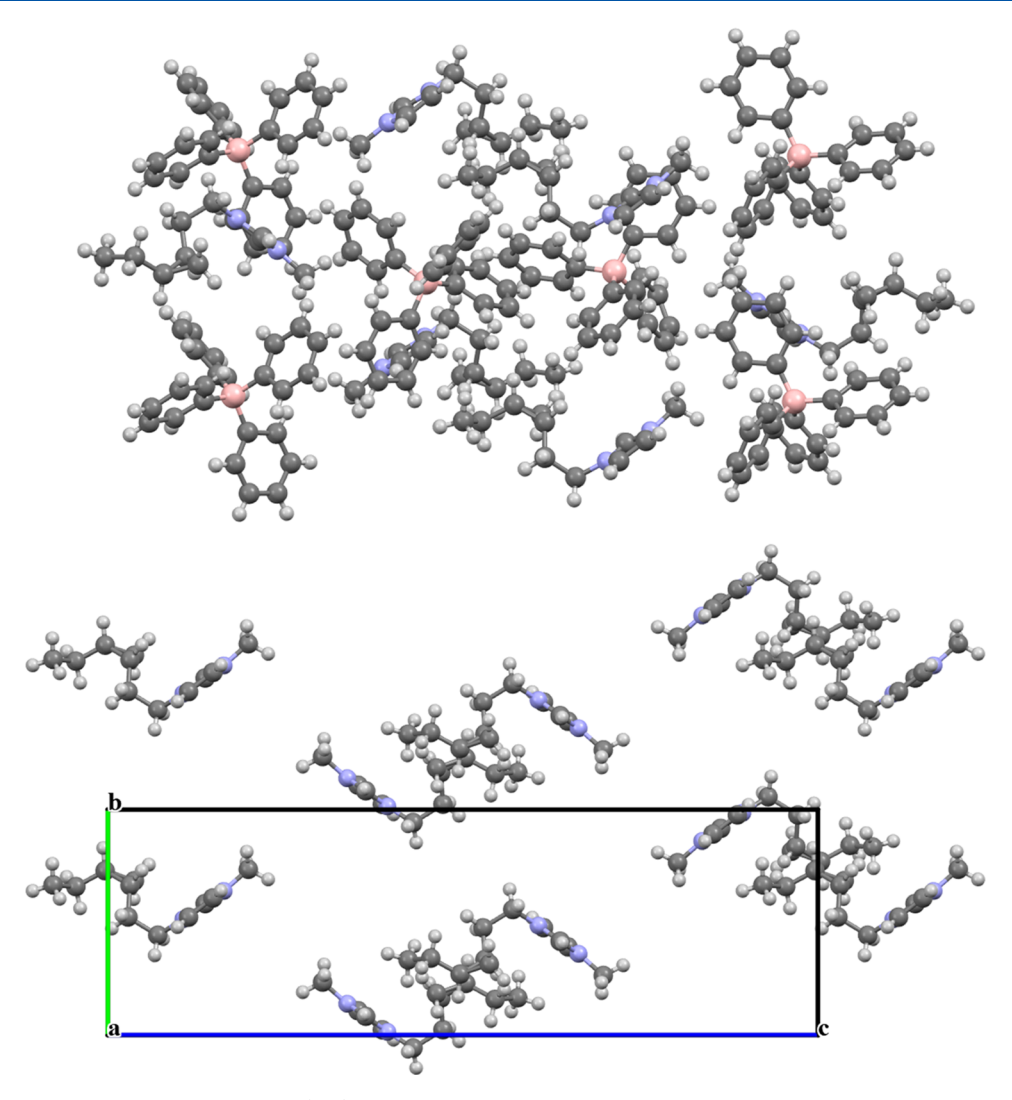


Figure 7. Packing diagram of compound 14-CP (top). Packing diagram viewed down the crystallographic b axis of just the cation. Disorder omitted for clarity (bottom).

apparent that the *gauche* conformation of the C7–C8–C9–C11 bonds produce a distinct kinking of the side chain in which it is incorporated (Figures 6 and 7). While this will, as demonstrated, lower the melting point, the introduction of new structural features of ILs also leads to the formation of new intermolecular interactions. Thus, an examination of the interactions and local structure of the cation is necessary to draw out the structural impacts of the introduction of the cyclopropyl motif to the side chains.

A single cation—anion pair exists in the asymmetric unit of compound 14-CP (Figure 6). The cation is disordered over three positions. This disorder, however, does offer insight into the solution structure of the IL (see Figure S1). First, the disorder in the alkyl chain of the cation arises predominantly from changes in the torsion angles of specific bonds. Following previously established nomenclature, 33 moieties A and C exist in the G/G conformation, while B is in the G'/G' conformation. These orientations are with respect to the N3–C7–C8–C9 and C7–C8–C9–C10 torsion angles. These energetically accessible changes in alkyl conformation, in conjunction with alkyl flexibility, play a key role in the phase transitions of ILs. 18,34 Second, additional changes in torsion angles are seen when examining the entire alkyl chain with

respect to the imidazolium headgroup. Specifically, moieties A and B show an $\sim 180^{\circ}$ rotation of the entire chain, wherein the cyclopropyl moieties are oriented in different directions (Figure 7). Thus, the inclusion of the cyclopropyl moiety does not appear to hinder the rotation of the chain as a whole. Finally, the ethyl portion of the chain, that is, C12 and C13, also shows distinct orientations. Three orientations of the ethyl group, with respect to the cyclopropyl moiety, are observed. Moiety A has a C9-C10-C11-C12 torsion angle of 81°, B is 148° , and C is -158° . In summary, three orientations of the alkyl chain are observed at multiple strategic points in the chain. These readily accessible torsion angles and chain conformations contribute to the lower lattice energy for the compound, decreasing the melting points of these ILs. It should be noted that the size of the anion is theorized to influence the orientation of the alkyl chains in ILs, and thus, changes are expected when contrasting the crystal (BPh₄⁻) vs the Tf₂N⁻ analogs.³⁵

An initial theoretical validation of the concept was provided by the computational study of the molecular structure of the 14-CP. Only the major portion of the disordered cation was optimized using the Spartan'20. Table 4 compares bond distances of the optimized and experimental structures, while

Table 4. List of the Bond Distances of the Optimized and Experimental Structures of 14-CP

| bond | experimental | calculated | difference |
|---------|--------------|------------|------------|
| N1-C2 | 1.322 | 1.332 | -0.010 |
| C2-N3 | 1.338 | 1.329 | 0.009 |
| N3-C4 | 1.370 | 1.377 | -0.007 |
| C4-C5 | 1.360 | 1.358 | 0.002 |
| C5-N1 | 1.387 | 1.378 | 0.009 |
| N1-C6 | 1.459 | 1.466 | -0.007 |
| N3-C7 | 1.472 | 1.475 | -0.003 |
| C7-C8 | 1.526 | 1.528 | -0.002 |
| C8-C9 | 1.502 | 1.512 | -0.010 |
| C9-C10 | 1.520 | 1.516 | 0.004 |
| C9-C11 | 1.507 | 1.508 | -0.001 |
| C10-C11 | 1.504 | 1.502 | 0.002 |
| C11-C12 | 1.497 | 1.512 | -0.015 |
| C12-C13 | 1.527 | 1.527 | 0.000 |

Figure S2 shows an overlay of the two structures highlighting the similarities in the two. It is well understood, however, that the structures within a crystal may not be at a global energy minima. Thus, we searched for the low-lying conformers to gain a better understanding of the different geometries this

cation may adopt. The seven lowest-energy conformers are shown in Figure 8 (I–VII). These conformers were chosen given that the change in energy between the conformers is \sim 5 kJ/mol, promoting flexibility within the lipid chains.

Several noteworthy observations are made regarding these theoretical structures. First, the two lowest-energy conformers are related by a simple rotation of the imidazolium ring, with the C2-H moieties oriented 180° with each other. Curiously, despite this simple change in orientation, II is slightly higher in energy than I ($\Delta E_{1-2} = 1.53$ kJ/mol). This does help explain the observed disorder in the crystal; however, wherein two portions of the disorder are related by the rotation of the ring. Second, conformational changes in the pendant ethyl chain of the cation are a point of distinction for several conformers (e.g., III vs IV). Again, the theoretical studies mirror what is observed experimentally with the disordered moieties in the crystal. Third, the alkyl chains in all of the conformers are in either the G or G' conformation, as observed in the crystal. Finally, conformer V is closest in overall structure when compared to the experimentally observed cation, with respect to the major portion of the disorder. Conformer VII matches well with the disordered portion C of the cation. Thus, the conformations found in the crystal are likely not the lowest energy. Based on these results, it is likely that many closely

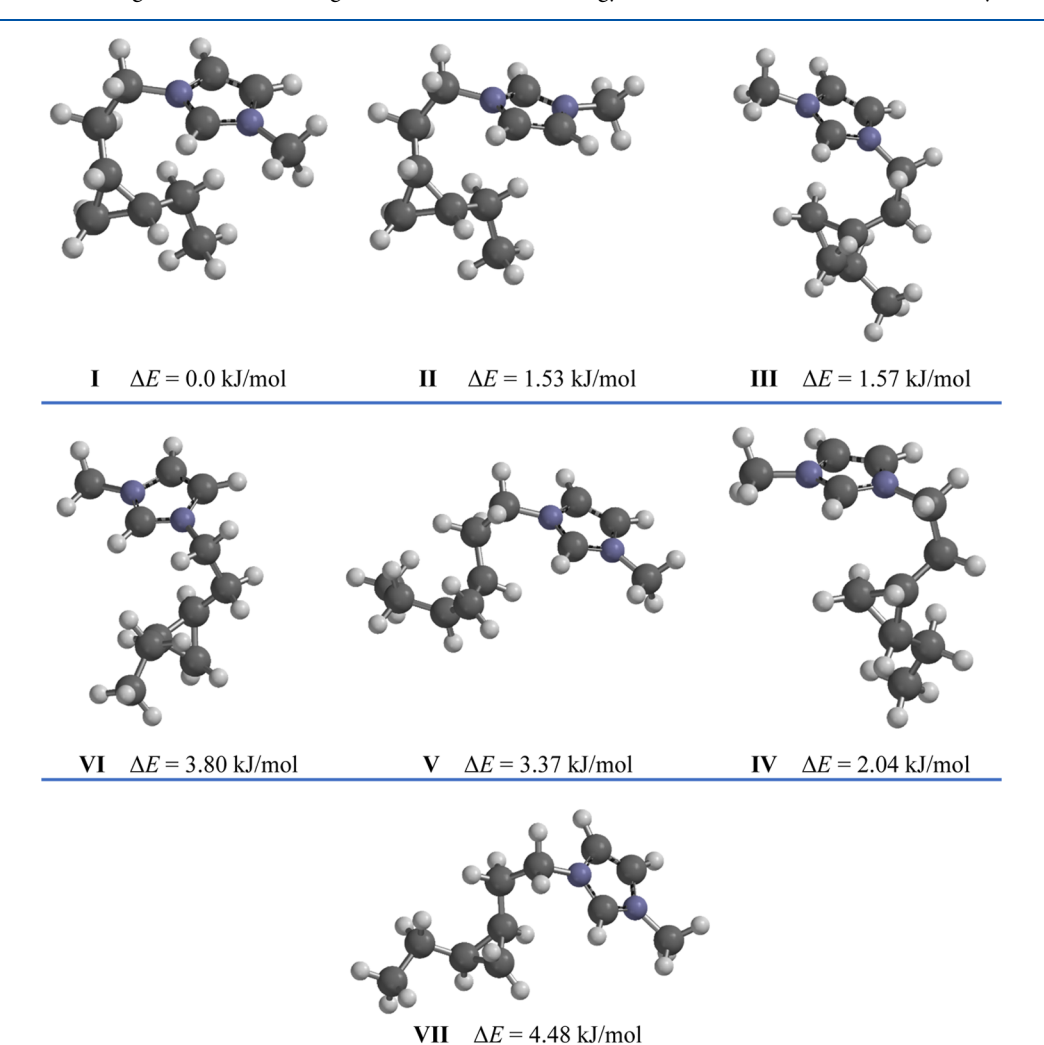


Figure 8. Seven lowest-energy conformers of the cation of compound 14-CP. Values shown depict the relative change in energy when compared with the lowest-energy conformer (I).

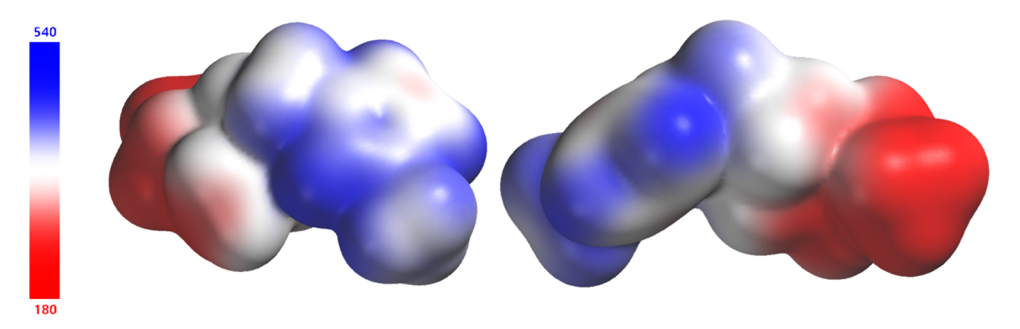


Figure 9. Cation of 14-CP mapped with the ESP. The two views show the different angles of the compound for clarity.

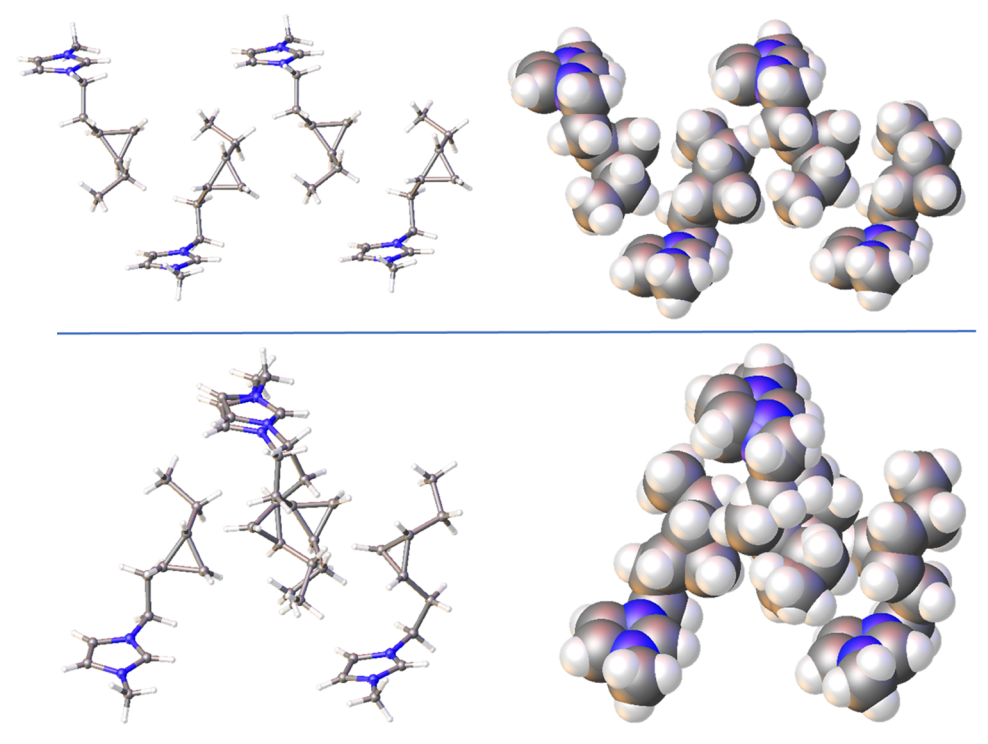


Figure 10. Depictions of the side-on (top) and face-on (bottom) interactions arising from the cyclopropyl moiety of the cation. Depictions with the van der Waals radii spheres are provided to show the $H \cdot \cdot \cdot H$ interactions.

related conformers are present in the liquid state of 14-CP, an important feature leading to the depressed melting point of these ILs. In particular, conformers I—IV show a distinctive arrangement of the cyclopropyl moiety with respect to the imidazolium core when compared with the crystalline molecules. This points to the possibility of rotation around this portion of the chain, *albeit* partially restricted due to the cyclical geometry.

To further understand the crystal structure and the interactions observed therein, we calculated the electrostatic potential map (ESP) 36 of the optimized structure (Figure 9). The features of the ESP are similar to other previously reported structures. 37 The cation shows the most positive regions of the surface with all three aromatic hydrogens being positive. C2–H is the most positive with V_{s,max} = 530 kJ/mol, as expected. Further, the aliphatic hydrogens near the imidazolium ring, C6 and C7, are also regions of positive density, accounting for some of the shorter hydrogen interactions observed in the crystal (vide infra). Finally, the tail-end of the alkyl chain and the cyclopropyl moiety are the more negative regions of the calculated ESP. This helps explain

the discussed cation-cation interactions observed in the crystal (vide supra).

While the local geometry of the cation provides useful information, the packing and long-range order of the crystal give relevant information with respect to interionic interactions. Examining the packing diagram for 14-CP reveals several notable features. First, the cation as a whole is surrounded by seven BPh₄ moieties (see Figure S3). Five of the anions surround the imidazolium ring, and the remaining two interact, predominantly, with the alkyl chains. Second, there are no π - π interactions between cations or anions, an important packing motif in imidazolium ILs.³⁸ Third, a close inspection of the images in Figure S3 reveals two regions near the cyclopropyl moiety in which cation—anion interactions are not observed. In fact, these atoms interact with symmetry adjacent cyclopropyl moieties of other cations.

Two cation—cation interaction motifs are observed when examining the interactions arising from the cyclopropyl moiety (Figure 10). These interactions arise from the different conformations of the alkyl chain (crystallographic disorder). The interactions can best be described as a side-on interaction with the cyclopropyl moiety and a face-on interaction. In both

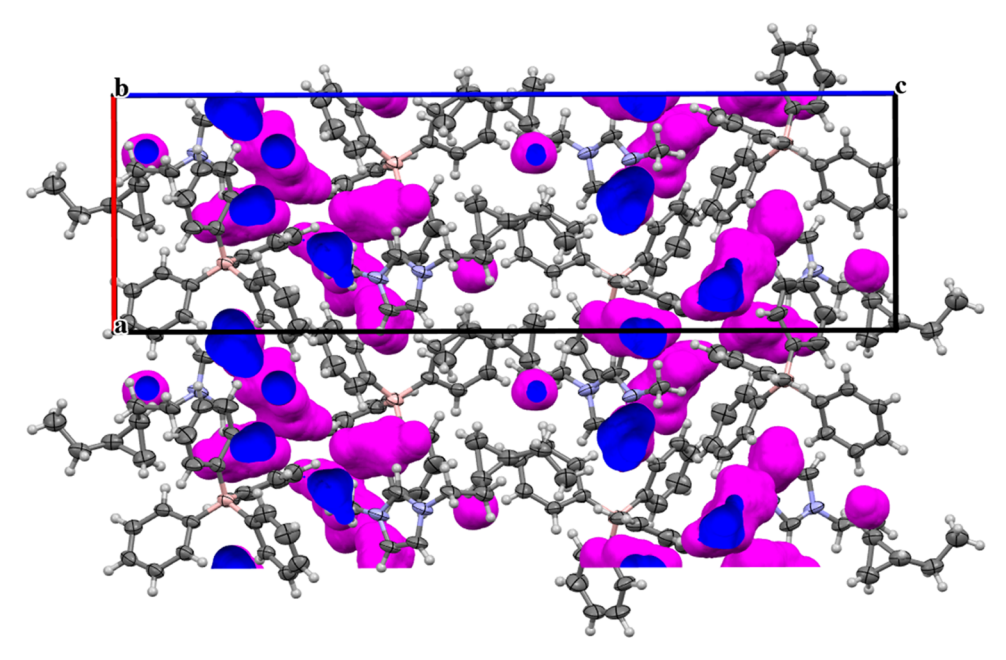


Figure 11. Depiction of the void space within the crystal of compound 14-CP. Disorder omitted for clarity within the image, but accounted for with the calculation of the voids.

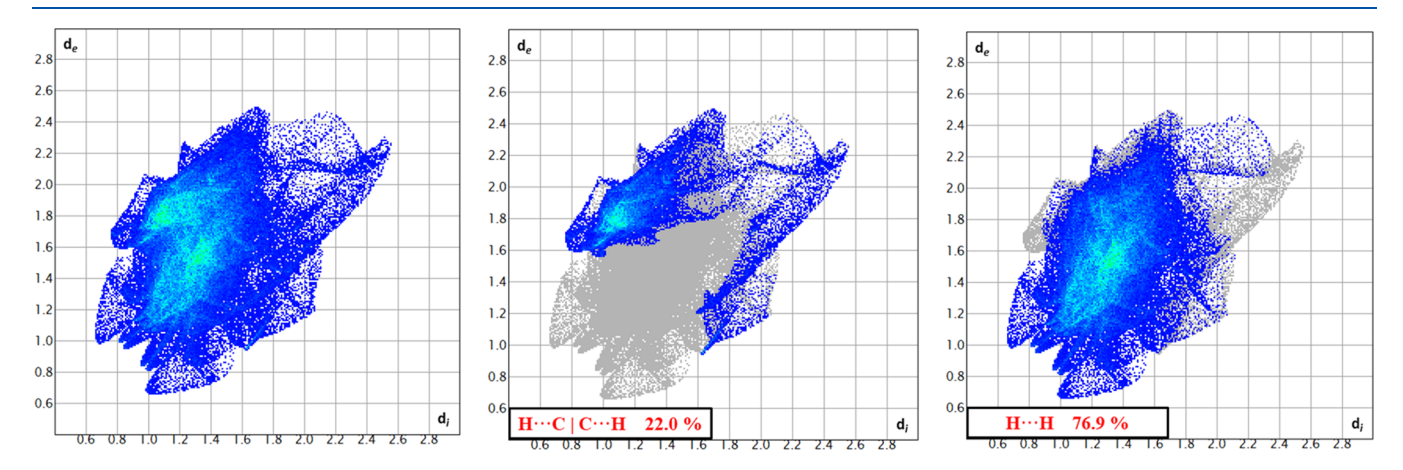


Figure 12. Complete fingerprint of the cation from compound 14-CP (left). Fingerprint showing the reciprocal H···ClC···H interactions of the cation (middle). Fingerprint showing the H···H interactions of the cation (right).

cases, the interactions are between the hydrogen atoms of the rings, accounting for a portion of the H···H interactions observed in the fingerprints (vide infra). These interactions with the cyclopropyl ring complement the computational studies, which revealed negative ESP in this region of the alkyl chain (vide supra).

To further examine the packing of the compounds, the crystalline voids were calculated and visualized (Figure 11). The total volume of the crystalline voids was found to be 160.72 ų or 5.6% of the unit cell volume. Voids are located predominantly near the faces of the Ph₄B⁻ anion. This follows the previous observation on the lack of any notable $\pi-\pi$ interactions in this structure. Additional voids are also seen above the face of the imidazolium ring. The lack of cation π interactions is significant, given the proposed importance of these interactions within ILs.^{39,40} However, it is likely that due to the bulky nature of the Ph₄B⁻ anion, efficient packing maximizing these π interactions is not achievable.

Hirshfeld surface analysis allows for a deeper understanding of the exact interactions present in the crystalline state.⁴¹ While

the overall interactions in the crystalline state of ILs are dominated by Coulombic interactions, other noncovalent interactions do play a role in the formation of the structure, ⁴² particularly with respect to directional interactions (e.g., hydrogen bonding, σ -hole interactions, etc. ⁴³). Further, these interactions will be present in the liquid state as well, ⁴⁴ thus knowledge of specific interactions can help find specialized applications for our compounds. The interaction fingerprints are shown in Figure 12, and the Hirshfeld surface mapped with d_{norm} , shape index, and the fragment patch are shown in Figure 13

Several important observations are made when examining the results of the Hirshfeld surface analysis. First, H···H interactions are the dominant noncovalent interactions within this crystal. Overall, hydrogen interactions account for almost 96% of the interionic interactions. This is expected, of course, given the composition of both the cation and anion. The geometries and nature of these H interactions are important; however, the remaining nonhydrogen interactions, 4% of the total interactions, are residual close contracts with carbon or

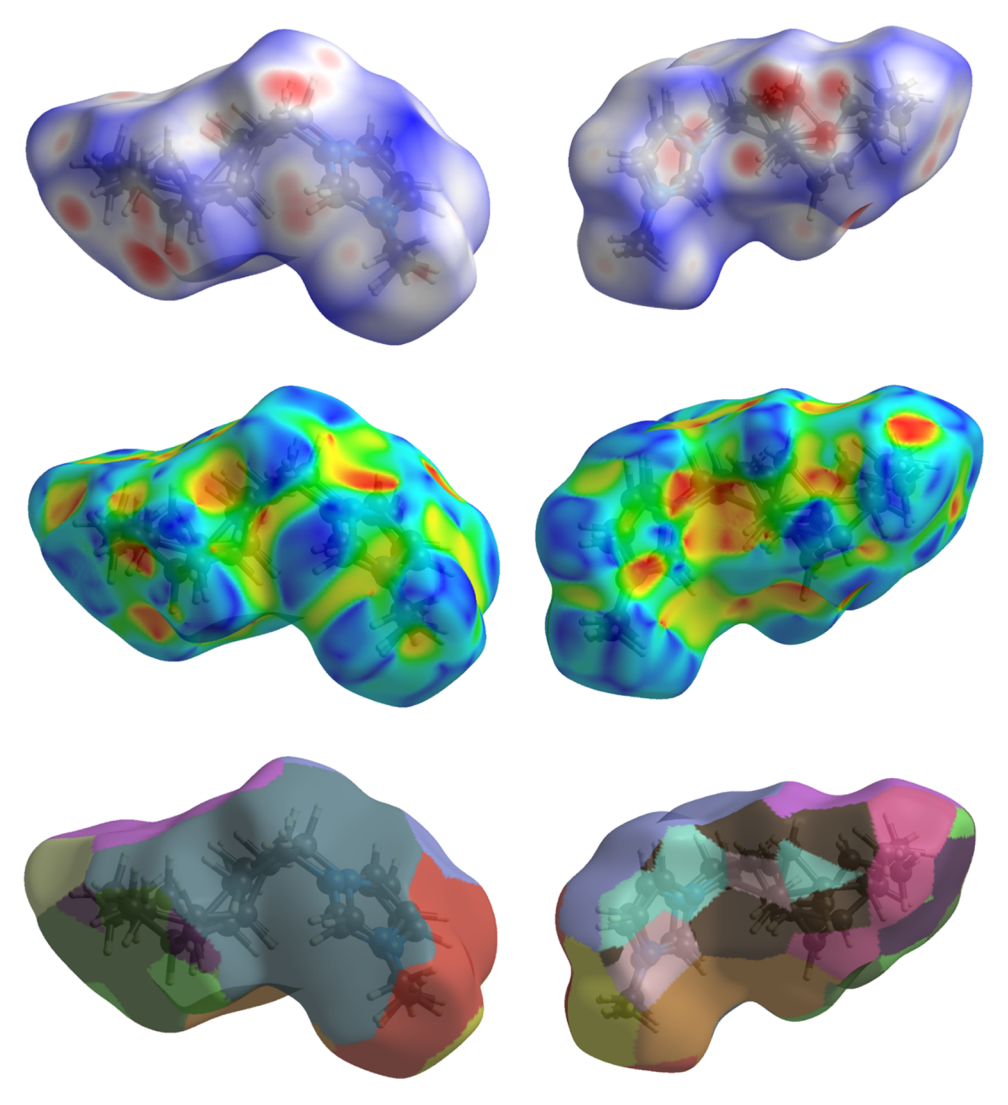


Figure 13. From top to bottom, the Hirshfeld surface of the cation from compound 14-CP mapped with d_{norm}, shape index, and fragment patch.

nitrogen atoms. Second, the dispersed regions of interactions on the periphery of the fingerprint are a consequence of the disorder of the alkyl chain. However, the dispersed points at the top right of the shape ($d_{\rm i} \approx d_{\rm e} \approx 2.5$ Å) are likely a consequence of inefficient packing of the ions.

Examining the specific hydrogen interactions, that is, H···C, H...N, H...H, offers insight into the classification of interactions present. While no π - π stacking is observed, $H \cdots \pi$ interactions are present. These are represented by the H···ClC···H fingerprints (Figure S4). These H··· π interactions account for 22.0% of the interactions. Close inspection of the fingerprint reveals an asymmetric shape of the plot. While some of this is due to the disorder, the interactions between different moieties are also present. For example, the upper region of the figure ($d_i = 1.0 \text{ Å}$, $d_e = 1.7 \text{ Å}$) is due to, predominantly, $H \cdots \pi$ interactions arising between the cation and anion (see Figure 10). Close inspection of Figure 10 reveals that all the aromatic hydrogens on the cation interact with symmetry adjacent π systems. Additionally, the methylene and methyl hydrogens on C6 and C7 are also interacting. This follows from the ESP discussion wherein the hydrogens on these carbons (e.g., C2-H, C4-H, C5-H, C6-H, C7-H) have the most positive potential.

Interactions arising from the cyclopropyl moiety involve both cation···cation and cation···anion interactions. As discussed previously, the cyclopropyl moiety does interact with the other cations through H···H interactions. These interactions are visualized as the four blunted spikes near the bottom left of the H···H fingerprint ($d_{\rm i} \approx d_{\rm e} \approx 1.0$ Å). Additional H···H interactions are observed between the cyclopropyl hydrogens and the anions. A depiction of these interactions is shown in Figure S5.

■ EXPERIMENTAL SECTION

The detailed synthetic procedure and the crystallographic and computational methods used in this work were described in the Supporting Information.

CONCLUSIONS

In this study, we demonstrated that ILs with long alkyl appendages respond to side-chain modification—specifically cyclopropanation—in a manner that mimics the mechanisms that underlie homeoviscous adaptation in living organisms. The introduction of the cyclopropyl moieties as the basis for developing new lipid-like ILs provides key insights into features that are consistent with achieving high fluidity in such materials, ones that are not evident from our previous

research. Comparison of the melting points of cyclopropanated ILs, saturated/unsaturated ILs (representative first-generation lipid-like ILs), and their ersatz fatty acids vs the structural variation among them allowed us to readily identify the key structure-property (T_m) relationships. The present data in Table 1 reveal distinct melting point depression and packing disruption in lipid-like ILs, based on the strategic introduction of the cyclopropyl motifs into the aliphatic side chain, although except in one case (2-CP), the degree of melting point depression (relative to saturated and unsaturated reference compounds) as great as that evoked by unsaturation. Interestingly, the $T_{\rm m}$ of 2-CP (having the lowest, cf. "best," $T_{\rm m}$ among the cyclopropanated ILs) with its C_{16} side chain is 13.0 °C lower than its unsaturated counterpart 2-AL (the "best" olefinic IL). In line with previously studied olefinic ILs, the cis cyclopropyl motif in the side chains of the new salts is in fact the most powerful downward driver of $T_{\rm m}$, relative to the trans isomer, although sub-ambient $T_{\rm m}$ values (e.g., 7-CP, 21.2 °C) can still be achieved.

Using X-ray crystallography and computational approaches, we found that cyclopropane-functionalized ILs tend to increase the fluidity of ILs by interfering with packing, forming *gauche* defects, and decreasing the chain orders. Within the crystal structure examination, it was found that multiple interaction motifs arising from the cyclopropyl moiety are evident; specifically, a face-on and side-on set of interactions between symmetry adjacent hydrogens. As a whole, however, the addition of a cyclopropane moiety follows previously observed trends for interactions arising from ILs. Remarkably, computational studies predicted that the room-temperature population of the *gauche* conformers ought to collectively comprise ca. 100% of the total conformer population around this linkage.

ASSOCIATED CONTENT

Supporting Information

The Supporting Information is available free of charge at https://pubs.acs.org/doi/10.1021/acs.jpcb.2c07872.

Synthesis and characterizations of the ILs; ¹H, and ¹³C NMR spectra; DSC and TGA thermograms; additional theoretical and crystallographic data (PDF)

Crystallographic data (CIF)

AUTHOR INFORMATION

Corresponding Authors

Richard A. O'Brien – Department of Chemistry, The University of South Alabama, Mobile, Alabama 36688, United States; Email: robrien@southalabama.edu

James H. Davis, Jr. – Department of Chemistry, The University of South Alabama, Mobile, Alabama 36688, United States; orcid.org/0000-0001-9573-3597; Email: jdavis@southalabama.edu

Arsalan Mirjafari — Department of Chemistry, State University of New York at Oswego, Oswego, New York 13126, United States; ◎ orcid.org/0000-0002-5502-0602; Email: arsalan.mirjafari@oswego.edu

Authors

Patrick C. Hillesheim – Department of Chemistry and Physics, Ave Maria University, Ave Maria, Florida 34142, United States; orcid.org/0000-0002-9567-4002

- Mohammad Soltani Department of Chemistry, The University of South Alabama, Mobile, Alabama 36688, United States
- Kelly J. Badilla-Nunez Department of Chemical and Biomolecular Engineering, The University of South Alabama, Mobile, Alabama 36688, United States
- Ben Siu Department of Chemical and Biomolecular Engineering, The University of South Alabama, Mobile, Alabama 36688, United States
- Muhammadiqboli Musozoda Department of Chemistry, State University of New York at Oswego, Oswego, New York 13126, United States
- Kevin N. West Department of Chemical and Biomolecular Engineering, The University of South Alabama, Mobile, Alabama 36688, United States; ◎ orcid.org/0000-0001-8503-4522

Complete contact information is available at: https://pubs.acs.org/10.1021/acs.jpcb.2c07872

Author Contributions

The manuscript was written through contributions of all authors, including conceptualization, original draft preparation, review, and editing. The project was designed by R.A.O., A.M., and J.H.D. Jr. The ILs were prepared by R.A.O. and M.S. Crystallographic and computational works were conducted by P.C.H. and M.M. Thermophysical data were collected by K.J.B.-N., B.S., and K.N.W. A.M., P.C.H., K.N.W., and J.H.D. Jr. wrote the manuscript. Funding acquisition was done by A.M. and J.H.D. Jr. All authors have given approval to the final version of the manuscript.

Notes

The authors declare no competing financial interest.

ACKNOWLEDGMENTS

This material is based upon work supported by the National Science Foundation under Grant Nos. CHE-1952846 and CHE-1464740. Acknowledgment is made by P.C.H. to the Donors of the American Chemical Society Petroleum Research Fund (66195-UNI10) for partial support of this research. A.M. is grateful to the Richard S. Shineman Foundation and the Oswego College Foundation for the generous financial support. P.C.H. would like to thank Michael and Lisa Schwartz for their generous financial support of the undergraduate research program.

■ REFERENCES

- (1) Welton, T. Ionic Liquids: A Brief History. *Biophys. Rev.* 2018, 10, 691–706.
- (2) Commercial Applications of Ionic Liquids. In *Green Chemistry and Sustainable Technology*; Shiflett, M. B., Ed.; Springer International Publishing, 2020.
- (3) Plechkova, N. V.; Seddon, K. R. Applications of Ionic Liquids in the Chemical Industry. *Chem. Soc. Rev.* **2008**, *37*, 123–150.
- (4) Wilkes, J. S.; Zaworotko, M. J. Air and Water Stable 1-Ethyl-3-Methylimidazolium Based Ionic Liquids. *J. Chem. Soc. Chem. Commun.* **1992**, *13*, 965–967.
- (5) Heintz, A. Recent Developments in Thermodynamics and Thermophysics of Non-Aqueous Mixtures Containing Ionic Liquids. A Review. *J. Chem. Thermodyn.* **2005**, *37*, 525–535.
- (6) Murray, S. M.; O'Brien, R. A.; Mattson, K. M.; Ceccarelli, C.; Sykora, R. E.; West, K. N.; Davis, J. H. The Fluid-Mosaic Model, Homeoviscous Adaptation, and Ionic Liquids: Dramatic Lowering of the Melting Point by Side-Chain Unsaturation. *Angew. Chem., Int. Ed.* **2010**, 49, 2755–2758.

- (7) Mirjafari, A.; O'Brien, R. A.; Murray, S. M.; Mattson, K. M.; Mobarrez, N.; West, K. N.; Davis, J. H. Lipid-Inspired Ionic Liquids Containing Long-Chain Appendages: Novel Class of Biomaterials with Attractive Properties and Applications; Visser, A. E.; Bridges, N. J.; Rogers, R. D., Eds.; ACS Symposium Series; American Chemical Society: Washington, DC, 2012; Vol. 1117, pp 199–216.
- (8) O'Brien, R. A.; West, C. W.; Hollingsworth, B. E.; Stenson, A. C.; Henderson, C. B.; Mirjafari, A.; Mobarrez, N.; West, K. N.; Mattson, K. M.; Salter, E. A.; Wierzbicki, A.; Davis, J. H. A Simple and Rapid Route to Novel Tetra(4-Thiaalkyl)Ammonium Bromides. *RSC Adv.* 2013, 3, 24612–24617.
- (9) Kwan, M.-L.; Mirjafari, A.; McCabe, J. R.; O'Brien, R. A.; Essi, D. F.; Baum, L.; West, K. N.; Davis, J. H. Synthesis and Thermophysical Properties of Ionic Liquids: Cyclopropyl Moieties versus Olefins as $T_{\rm m}$ -Reducing Elements in Lipid-Inspired Ionic Liquids. *Tetrahedron Lett.* **2013**, 54, 12–14.
- (10) Mirjafari, A.; O'Brien, R. A.; West, K. N.; Davis, J. H. Synthesis of New Lipid-Inspired Ionic Liquids by Thiol-Ene Chemistry: Profound Solvent Effect on Reaction Pathway. *Chem. Eur. J.* **2014**, *20*, 7576–7580.
- (11) O'Brien, R. A.; Zayas, M. S.; Nestor, S. T.; Gaitor, J. C.; Paul, L. M.; Edhegard, F. A.; Minkowicz, S.; Sykora, R. E.; Sheng, Y.; Michael, S. F.; Isern, S.; Mirjafari, A. Biomimetic Design of Protic Lipidic Ionic Liquids with Enhanced Fluidity. *New J. Chem.* **2016**, *40*, 7795–7803.
- (12) Gaitor, J. C.; Paul, L. M.; Reardon, M. M.; Hmissa, T.; Minkowicz, S.; Regner, M.; Sheng, Y.; Michael, S. F.; Isern, S.; Mirjafari, A. Ionic Liquids with Thioether Motifs as Synthetic Cationic Lipids for Gene Delivery. *Chem. Commun.* **2017**, *53*, 8328–8331
- (13) Philippi, F.; Welton, T. Targeted Modifications in Ionic Liquids from Understanding to Design. *Phys. Chem. Chem. Phys.* **2021**, 23, 6993–7021.
- (14) Gordon, C. M.; Holbrey, J. D.; Kennedy, A. R.; Seddon, K. R. Ionic Liquid Crystals: Hexafluorophosphate Salts. *J. Mater. Chem.* **1998**, *8*, 2627–2636.
- (15) Bradley, A. E.; Hardacre, C.; Holbrey, J. D.; Johnston, S.; McMath, S. E. J.; Nieuwenhuyzen, M. Small-Angle X-Ray Scattering Studies of Liquid Crystalline 1-Alkyl-3-Methylimidazolium Salts. *Chem. Mater.* **2002**, *14*, 629–635.
- (16) López-Martin, I.; Burello, E.; Davey, P. N.; Seddon, K. R.; Rothenberg, G. Anion and Cation Effects on Imidazolium Salt Melting Points: A Descriptor Modelling Study. *ChemPhysChem* **2007**, *8*, 690–695.
- (17) Hayes, R.; Warr, G. G.; Atkin, R. Structure and Nanostructure in Ionic Liquids. *Chem. Rev.* **2015**, *115*, 6357–6426.
- (18) Bernardino, K.; Zhang, Y.; Ribeiro, M. C. C.; Maginn, E. J. Effect of Alkyl-Group Flexibility on the Melting Point of Imidazolium-Based Ionic Liquids. *J. Chem. Phys.* **2020**, *153*, No. 044504.
- (19) Cimini, A.; Palumbo, O.; Trequattrini, F.; Paolone, A. Influence of the Alkyl Chain Length on the Low Temperature Phase Transitions of Imidazolium Based Ionic Liquids. *J. Solution Chem.* **2022**, *51*, 279–295.
- (20) Ji, Y.; Shi, R.; Wang, Y.; Saielli, G. Effect of the Chain Length on the Structure of Ionic Liquids: From Spatial Heterogeneity to Ionic Liquid Crystals. *J. Phys. Chem. B* **2013**, *117*, 1104–1109.
- (21) Blanco-Díaz, E.; González-Alatorre, G.; Lona-Ramírez, F. J.; Castrejón-González, E. O. Effect of Increasing the Cation Chain Length on Thermodynamic and Transport Properties of Ionic Liquids Using Molecular Dynamics. *J. Mol. Liq.* **2021**, 334, No. 116430.
- (22) Mirjafari, A.; O'Brien, R. A.; Davis, J. H. Synthesis and Properties of Lipid-Inspired Ionic Liquids. In *Ionic Liquids in Lipid Processing and Analysis*; Elsevier, 2016; pp 205–223.
- (23) Sinensky, M. Homeoviscous Adaptation-A Homeostatic Process That Regulates the Viscosity of Membrane Lipids in Escherichia Coli. *Proc. Natl. Acad. Sci. U.S.A.* 1974, 71, 522–525.
- (24) O'Brien, R. A.; Mirjafari, A.; Jajam, V.; Capley, E. N.; Stenson, A. C.; West, K. N.; Davis, J. H. Functionalized Ionic Liquids with Highly Polar Polyhydroxylated Appendages and Their Rapid

- Synthesis via Thiol-Ene Click Chemistry. *Tetrahedron Lett.* **2011**, 52, 5173–5175.
- (25) O'Brien, R. A.; Mirjafari, A.; Mattson, K. M.; Murray, S. M.; Mobarrez, N.; Salter, E. A.; Wierzbicki, A.; Davis, J. H.; West, K. N. The Effect of the Sulfur Position on the Melting Points of Lipidic 1-Methyl-3-Thiaalkylimidazolium Ionic Liquids. *J. Phys. Chem. B* **2014**, *118*, 10232–10239.
- (26) Grogan, D. W.; Cronan, J. E. Cyclopropane Ring Formation in Membrane Lipids of Bacteria. *Microbiol. Mol. Biol. Rev.* **1997**, *61*, 429–441.
- (27) Inuki, S.; Fujimoto, Y. Total Synthesis of Naturally Occurring Chiral Cyclopropane Fatty Acids and Related Compounds. *Tetrahedron Lett.* **2019**, *60*, 1083–1090.
- (28) Cruz-Morales, P.; Yin, K.; Landera, A.; Cort, J. R.; Young, R. P.; Kyle, J. E.; Bertrand, R.; Iavarone, A. T.; Acharya, S.; Cowan, A.; Chen, Y.; Gin, J. W.; Scown, C. D.; Petzold, C. J.; Araujo-Barcelos, C.; Sundstrom, E.; George, A.; Liu, Y.; Klass, S.; Nava, A. A.; Keasling, J. D. Biosynthesis of Polycyclopropanated High Energy Biofuels. *Joule* 2022, 6, 1590–1605.
- (29) Poger, D.; Mark, A. E. A Ring to Rule Them All: The Effect of Cyclopropane Fatty Acids on the Fluidity of Lipid Bilayers. *J. Phys. Chem. B* **2015**, *119*, 5487–5495.
- (30) Nan, H.; Zhang, C.; O'Brien, R. A.; Benchea, A.; Davis, J. H.; Anderson, J. L. Lipidic Ionic Liquid Stationary Phases for the Separation of Aliphatic Hydrocarbons by Comprehensive Two-Dimensional Gas Chromatography. *J. Chromatogr. A* **2017**, *1481*, 127–136.
- (31) Silvius, J. R.; McElhaney, R. N. Effects of Phospholipid Acylchain Structure on Thermotropic Phase Properties. 2: Phosphatidylcholines with Unsaturated or Cyclopropane Acyl Chains. *Chem. Phys. Lipids* **1979**, *25*, 125–134.
- (32) Mirjafari, A. Ionic Liquid Syntheses via Click Chemistry: Expeditious Routes toward Versatile Functional Materials. *Chem. Commun.* **2018**, *54*, 2944–2961.
- (33) Saouane, S.; Norman, S. E.; Hardacre, C.; Fabbiani, F. P. A. Pinning down the Solid-State Polymorphism of the Ionic Liquid [Bmim][PF₆]. *Chem. Sci.* **2013**, *4*, 1270.
- (34) Endo, T.; Hoshino, S.; Shimizu, Y.; Fujii, K.; Nishikawa, K. Comprehensive Conformational and Rotational Analyses of the Butyl Group in Cyclic Cations: DFT Calculations for Imidazolium, Pyridinium, Pyrrolidinium, and Piperidinium. *J. Phys. Chem. B* **2016**, *120*, 10336–10349.
- (35) Winterton, N. Crystallography of Ionic Liquids. In *Ionic Liquids Completely Uncoiled*; John Wiley & Sons, Ltd., 2015; pp 231–534.
- (36) Murray, J. S.; Politzer, P. The Electrostatic Potential: An Overview. WIREs Comput. Mol. Sci. 2011, 1, 153–163.
- (37) Hunt, P. A.; Kirchner, B.; Welton, T. Characterising the Electronic Structure of Ionic Liquids: An Examination of the 1-Butyl-3-Methylimidazolium Chloride Ion Pair. *Chem. Eur. J.* **2006**, *12*, 6762–6775.
- (38) Matthews, R. P.; Welton, T.; Hunt, P. A. Competitive π Interactions and Hydrogen Bonding within Imidazolium Ionic Liquids. *Phys. Chem. Chem. Phys.* **2014**, *16*, 3238–3253.
- (39) García-Saiz, A.; de Pedro, I.; Migowski, P.; Vallcorba, O.; Junquera, J.; Blanco, J. A.; Fabelo, O.; Sheptyakov, D.; Waerenborgh, J. C.; Fernández-Díaz, M. T.; Rius, J.; Dupont, J.; Gonzalez, J. A.; Fernández, J. R. Anion– π and Halide–Halide Nonbonding Interactions in a New Ionic Liquid Based on Imidazolium Cation with Three-Dimensional Magnetic Ordering in the Solid State. *Inorg. Chem.* **2014**, 53, 8384–8396.
- (40) Schottel, B. L.; Chifotides, H. T.; Dunbar, K. R. Anion- π Interactions. *Chem. Soc. Rev.* **2008**, *37*, 68–83.
- (41) Spackman, M. A.; Jayatilaka, D. Hirshfeld Surface Analysis. CrystEngComm 2009, 11, 19–32.
- (42) Dunitz, J. D.; Gavezzotti, A.; Rizzato, S. "Coulombic Compression", a Pervasive Force in Ionic Solids. A Study of Anion Stacking in Croconate Salts. *Cryst. Growth Des.* **2014**, *14*, 357–366.

- (43) Braga, D.; Bazzi, C.; Grepioni, F.; Novoa, J. J. Electrostatic Compression on Non-Covalent Interactions: The Case of π Stacks Involving Ions. *New J. Chem.* **1999**, 23, 577–579.
- (44) Consorti, C. S.; Suarez, P. A. Z.; de Souza, R. F.; Burrow, R. A.; Farrar, D. H.; Lough, A. J.; Loh, W.; da Silva, L. H. M.; Dupont, J. Identification of 1,3-Dialkylimidazolium Salt Supramolecular Aggregates in Solution. *J. Phys. Chem. B* **2005**, *109*, 4341–4349.

□ Recommended by ACS

Crystallization Temperature, Vapor Pressure, Density, Viscosity, Specific Heat Capacity, and Corrosivity of the LiNO₃-DEG/H₂O Ternary System

Fangyan Xiang, Qingquan Su, et al.

JANUARY 31, 2023

JOURNAL OF CHEMICAL & ENGINEERING DATA

READ 🗹

Synthesis, Characterization, Pharmacogenomics, and Molecular Simulation of Pyridinium Type of Ionic Liquids and Their Applications

Ramalingam Tamilarasan, Amanullah Mohammed, et al.

JANUARY 16, 2023

ACS OMEGA

READ **'**

Base-Free Transfer Hydrogenation Catalyzed by Ruthenium Hydride Complexes of Coumarin-Amide Ligands

Samanta Yadav and Rajeev Gupta

MAY 25, 2023

ACS SUSTAINABLE CHEMISTRY & ENGINEERING

READ 🗹

Effect of Hydrogen Bonds on ${\rm CO_2}$ Capture by Functionalized Deep Eutectic Solvents Derived from 4-Fluorophenol

Zonghua Wang, Dezhong Yang, et al.

APRIL 07, 2023

ACS SUSTAINABLE CHEMISTRY & ENGINEERING

READ 🗹

Get More Suggestions >